ISSN: 0067-2904

Anticancer Mechanisms of Zoledronic Acid-Based Graphene Oxide Nanoparticles for Prostate Cancer Bone Metastases Treatment

Rasha Alsahlanee[1], Hala Abdulkareem Rasheed*[1], Hydar Muhsin Khalfa[2]
[1]*Department of Biotechnology, College of Science, University of Baghdad, Bagdad, Iraq*
[2]*Department of Biology, College of Science, University of Kufa, Al- Najaf, Iraq*

Received: 26/6/2022 Accepted: 15/8/2022 Published: 30/10/2022

Abstract:
Bone metastases are the main reason for death in males suffering from advanced prostate cancer. This study aimed to create zoledronic acid and graphene oxide conjugation for anticancer therapy. The process of conjugation was confirmed by several characterization methods including UV-VIS spectrophotometry, Fourier Transform Infrared Spectroscopy (FTIR), and atomic force microscope (AFM). the cytotoxicity of 400, 600, and 800 µg/ml to each GO, ZOL, and ZOL-GO was evaluated on a human hepatic cell line (WRL 68) and human prostate cancer cell line (PC3) using an MTT assay. The antitumor mechanisms of ZOL-GO were examined by cell cycle analysis. The results demonstrated That ZOL-GO caused a reduction in the cell viability of WRL 68 and PC3, with IC50 values of about 932.9 and 787.9 µg/ml respectively. The cell cycle distribution was evaluated after treating the prostate cancer cells (PC3) with 800µg/mL of ZOL-GO, the results showed the presence of a highly significant arresting effect in the G1 phase ($P \leq 0.002$) than the untreated cells (control). Our findings demonstrate the potential antitumor activity of using GO as a nanocarrier to improve the therapeutic efficacy of prostate cancer.

Keywords: PC3 cell line, antitumor, cell cycle, chemotherapy, drug delivery

الميكانيكية المضادة للسرطان لحامض الزولدرونك المرتبط بالجسيمات النانوية لاوكسيد الجرافين لعلاج سرطان البروستات المنتشر في العظم

رشا طالب عبد الله[1] , حلا عبد الكريم رشيد[2*] , حيدر محسن خلف[2]
[1]التقنيات الاحيائية, كلية العلوم, جامعة بغداد, بغداد, العراق
[1]علوم حياة, كلية العلوم, جامعة الكوفة, النجف, العراق

الخلاصه
النقائل العظمية هي سبب رئيسي للوفاة عند الذكوراللذين يعانون من سرطان البروستات المتقدم. هدفت هذه الدراسة إلى إنشاء اقتران حمض الزوليدرونيك وأكسيد الجرافين لعلاج السرطان. وقد تم تأكيد عملية الاقتران من خلال العديد من طرق التوصيف بما في ذلك قياس الطيف الضوئي بالأشعة المرئية وفوق البنفسجية (FTIR) ، والتحليل الطيفي للأشعة تحت الحمراء لتحويل فوريية ،ومجهر القوة الذرية (AFM). تم تقييم السمية الخلوية للتراكيز 400, 600, and 800 µg/ml لكل من GO و ZOL و ZOL–GO

*Email: hala.aljendeel@gmail.com

PC3)و الخط الخلوي لسرطان البروستات للانسان ( )68 WRL على الخط الخلوي لخلايا كبد الانسان (
من خلال تحليل دورة الخلية. أظهرت ZOL−GO تم فحص آليات مضاد الأورام لـ MTT باستخدام اختبار
تبلغ IC_{50} ، مع قيمPC3 و 68 WRL تسبب في انخفاض قابلية بقاء الخلية لـ ZOL−GO النتائج أن
حوالي 932.9 و 787.9 ميكروغرام / مل على التوالي. تم تقييم توزيع دورة الخلية بعد معالجة خلايا سرطان
، وأظهرت النتائج وجود تأثير توقيف مهم ZOL−GO مع 800 ميكروغرام / مل من (PC3) البروستات
مقارنة مع الخلايا غير المعالجة (السيطرة). توضح النتائج التي (P≤ 0.002) G1للغاية في المرحلة
كحامل نانوي لتحسين الفعالية العلاجية للبروستاتGOتوصلنا إليها النشاط المضاد للورم المحتمل لاستخدام

1. Introduction

Bone metastasis is a malignant condition that greatly reduces the patient's chances of survival [1-3]. Chemotherapy is one of the most successful therapies for bone metastasis [4]. An effective bisphosphonate medicine, Zoledronic acid (ZOL) reduces the level of tumor cells while also inhibiting the resorption of bone, making it an ideal treatment for cancer patients. [5, 6]. Due to the kidney's ability to more effectively filter ZOL particles, greater doses of the drug are required [7]. Because the complex size will rise when a sufficient drug carrier is used, the rate at which the medication is filtered through the kidneys will be slowed down, and as a result, it will take longer for the medication to be absorbed into the body. [5]. In addition to this, the medication is released from the drug carrier systems at a slower rate, which decreases the likelihood of unpleasant adverse effects occurring. These side effects are typically brought on by the condition of elevated dosages of the administered drug.[8]. Drug carriers for several anti-cancer treatments have been developed using graphene oxide, often known as GO, which is a layer of graphene that is one atom thick. The acronym GO is most often abbreviated to simply GO. The chemical structures of GO nanoparticles and ZOL both contain aromatic rings, making it possible for ZOL to form conjugates with GO through noncovalent interactions. In addition to stacking, hydrophobic interactions and hydrogen bonding are two more types of connections that can occur.[1]. Metastasis (cancer spreading to bones from many other organs such as the kidney, lung, thyroid, and especially the breast and prostate) occurs in about 70% of people with primary bone cancer. [6]. Using bisphosphonates as a metastatic treatment has been common practice for decades [6, 9-12]. A newer bisphosphonate, Zoledronic acid (ZOL), appears to be better at treating metastasis. [13-16] It's still difficult to use small ZOL particles here since the free drug is easily filtered before it gets to the tumor. [17, 18]. Because of this, it is necessary to administer bigger doses of the drug, which, in turn, raises the probability that undesirable side effects will become apparent. Acute inflammatory response, osteonecrosis of the jawbone, kidney failure, renal disease, electrolyte imbalance, and corneal inflammation are all potential side effects of this medication.[19-21]. Many different types of drug delivery systems are available, including poly(lactide-co-glycolide)[22], folates targeting liposome [23], -tricalcium phosphates[24], hydroxy-apatite[25], and gelatine[26], can be used to boost the effectiveness of ZOL and reduce the risk of adverse effects. High surface area, biocompatibility, and chemical modifiability of carbon allotropes make them promising candidates as drug carriers that can be used in place of traditional ones. [27]. Particularly, Drugs can be transported to cancer cells more effectively with the help of graphene tubes (CNT), graphene oxide (GO), carbon black, and nanodiamonds, among other materials [28]. In addition to these carbons, graphite oxide (GO) is distinguished by a number of apparent advantages, some of which are low production cost, and the existence of two exterior chemically reactive surfaces, the ease with which it can be manufactured and modified, as well as the complete absence of potentially hazardous metallic particles during its manufacture [29]. According to the findings of some studies [30, 31], the capacity of loading that GO possesses is larger than that of CNT. In addition to this, it has been discovered that CNT and carbon black have a higher degree of cytotoxicity than GO

does [15]. Because of this fact, the researchers that participated in this study concluded that GO would be the most suitable carrier for ZOL. Graphene in its oxidized state is referred to as GO, and it can be functionalized with a variety of groups, including hydroxyls, diols, epoxides, carboxyl, and ketones [32]. With the assistance of GO acting as a drug delivery carrier, anti-cancer medications such as doxorubicin [33], camptothecin [34], paclitaxel [35], pirfenidone [36], and Adriamycin [7, 34, 37] have been transported across the body with the help of GO as a drug carrier. The purpose of the current work was to conjugate the nanoparticles GO with the ZOL, describe these conjugates, and examine the possible anticancer impact as cytostatic agents in the treatment of prostate cancer bone metastases. In addition to this, one of our goals was to investigate the underlying processes that are responsible for the antitumor impact.

Materials and Methods

ZOL, GO and complexes Preparation

Making ZOL samples required mixing 5 ml of ultra-pure water with 2 mg/ml of zoledronic acid monohydrate (Sigma-Aldrich, >98 percent, HPLC) as a stock solution. The stock solution was then diluted by DMEM (Dulbecco's Modified Eagle Medium) and stirred overnight with a magnet (Isolab-340) to produce three separate samples with concentrations of 12.5, 50, and 200 M. The stock solution was prepared by mixing 4.5 ml of ultra-pure water with 0.5 ml of GO (Sigma-Aldrich, 2 mg/ml, the average diameter of a sheet: 22 m) and agitating it with a vortex at room temperature for 30 minutes in order to make varied concentrations of GO. After diluting the standard solutions with DMEM, a sonicator was used to stir for 30 minutes, yielding GO concentrations of 11, 7, 2, 91, and 0, 73 ng/ml. As revealed in Table 1, the GO and ZOL suspensions were then combined to form ZOL-GO complexes with various components. To prepare the stock solutions, DMEM was added, and the mixture was sonicated for fifteen minutes, but then agitated with a magnet overnight to get the desired concentrations of GO and ZOL in the suspensions.

Table 1: The composition of several ZOL-GO samples was determined.

Conjugation of zoledronic with graphene oxide	Graphene oxide ng ml^{-1}	Zoledronic acid (micromolar)
First sample	11.7	200
Second sample	2.91	50
Third sample	0.73	12.5

Conjugation characterization

UV-VIS spectrophotometer

1.25 mg/ml zoledronic acid, 0.25 mg/ml graphene oxide, and 1.25 mg/ml Zoledronic-Graphene combination were generated in ultrapure water. UV vis spectrophotometer examined ZOL-GO combination (Nanodrop Spectrophotometer, Thermo Technical, USA) [1]

Fourier transforms infrared

FTIR Instruments were used to examine the chemical properties of ZOL conjugated with Go in the spectrum of 4000–400 cm^{-1} at a frequency of 2 cm^{-1}. The ZOL-GO therapeutic complexes' efficacy was examined in cell culture experiments using PC3 cells and WRL 68 cells [20].

Atomic force microscope

This technique investigated GO and ZOL-GO nanoparticle surface morphology using the Inc. SPM-AA300 (U.S.). 5 droplets of GO and ZOL-GO nanoparticle solution were roasted at 110 °C for 30 minutes. The probe force on the sample surface can be utilized to continually screen the sample's 3D morphology/topography. This technique involves making a raster scan of the tested material while considering distance and force. For unique sample topography, the sample-tip force must be carefully considered [38].

Cell Culture

Human hepatic cell line (WRL68) and prostate cancer cell line (PC-3) were collected from Al-Nahrain University's biotechnology center- Baghdad, Iraq. Among the cancer cells, bone metastases are common. We employed DMEM along with fetal bovine serum (10%), and 100 U/mL of both penicillin, and streptomycin to keep these cell lines alive. Dulbecco's Modified Eagle Medium Temperatures of 37 degrees Celsius and 5% CO2 were decided upon for all cell lines. There have been investigations on cell survival, multiplication, and colony formation in passages as small as 10 [39, 40]

cell viability assessment

According to Ulukaya and colleagues' findings, the MTT assay was used to evaluate how the ZOL-GO drug complexes affected the viability of the cells [41]. To summarize, 2.5 x 10^3 cells were planted into 96-well plates, then placed inside the incubator at 37 degrees Celsius for 24 hours to facilitate attachment. On the next day, various concentrations (400, 600, and 800 µg/ml) of GO, ZOL and ZOL-GO were applied to the connected cells in order to treat them. There were three separate sets of tests conducted for each concentration. After a treatment period of 72 hours, DMEM was withdrawn from each well, and then 0.5 mg/ml of MTT solution was applied. The newly generated formazan crystals were dissolved in DMSO (170 µL /well) following an incubation period of 4 hours at 37 degrees Celsius. Afterwards, the plates were subjected to mechanical agitation for ten minutes, and the optical density was established using the microplate reader at 575 nm (Bio-rad, Germany). A log dosage inhibition curve was utilized in the analysis, to determine the IC50 values of the samples.

Cell Cycle Study

A commercial Cycle Test (TM plus DNA kit) was also used to investigate the FTC-133 cell cycle following the injection of ZOL-GO (BD Bioscience). Assays were carried out in Malaysia at the University of Malaya's Natural Products Research and Drug Discovery Center. Human prostatic cancerous cells that pre-treated with ZOL-GO at concentrations (400, 600, and 800 µg/ml, sequentially) for a time of 72 h were collected and placed in 70% ethanol at temperature of -4 °C overnight. The cells were subsequently treated using 50 mg/mL PI staining liquid together with 0.1 mg/mL RNase A at room temperature within 30 minutes in the dark. A flow cytometer and Multicycle software system (Beckman Colter, Brea, CA) was used to examine the DNA content of these cells[42].

Data Acquisition and Analysis

BD FACS flow cytometers are equipped with linear fluorescence magnification and forward scattering (FSC) and on the side-scatter (SSC) monitoring. A flow cytometer equipped together with an argon-particle laser illuminating at wavelength 488 nm excited PI in the dark blue-to-green scale. The sample was processed at a minimum absorption rate of 60 cycles per second, and the histograms were examined using the appropriate DNA analyzer.

Examining the data statistically

GraphPad, version 6.0, was used to do the statistical analysis in the data (USA). The records are stated as the means multiplied by the standard variation. (mean ± SD). There were noticeable variances between the groups. A one- or two-way Student's t analysis was utilized to evaluate the data ANOVA, if necessary. P value below than or equal to 0.05 was evaluated significantly.

2. RESULTS AND DISCUSSION

Photonic characterization of the ZOL-GO complex

The FTIR spectral data of GO as well as the ZOL-GO complex were generated at concentrations ranging from 200 ng/ml to 11.7 ng/ml as revealed in Figure1. The stretching mode of O-H [43, 44] can be identified in the FTIR spectra of GO by the bands located at 3562, 3465,1631,1224cm-1. There may be a connection between the band at1610 cm-1 and the C=O bending mode originated from the carboxyl group [43-46]. At a frequency of 1393 (38,39), the O-H distortion band was located. It is possible that the C-O functional group [44] was responsible for the formation of the band at 1083 cm-1. In addition, the band that is located at 918 cm-1 may be attributed to the presence of epoxy groups in the structure of GO [45, 46]. In the ZOL-GO spectra, the bands located at 3334 and 3292 cm-1 were related to O-H groups [43-46].

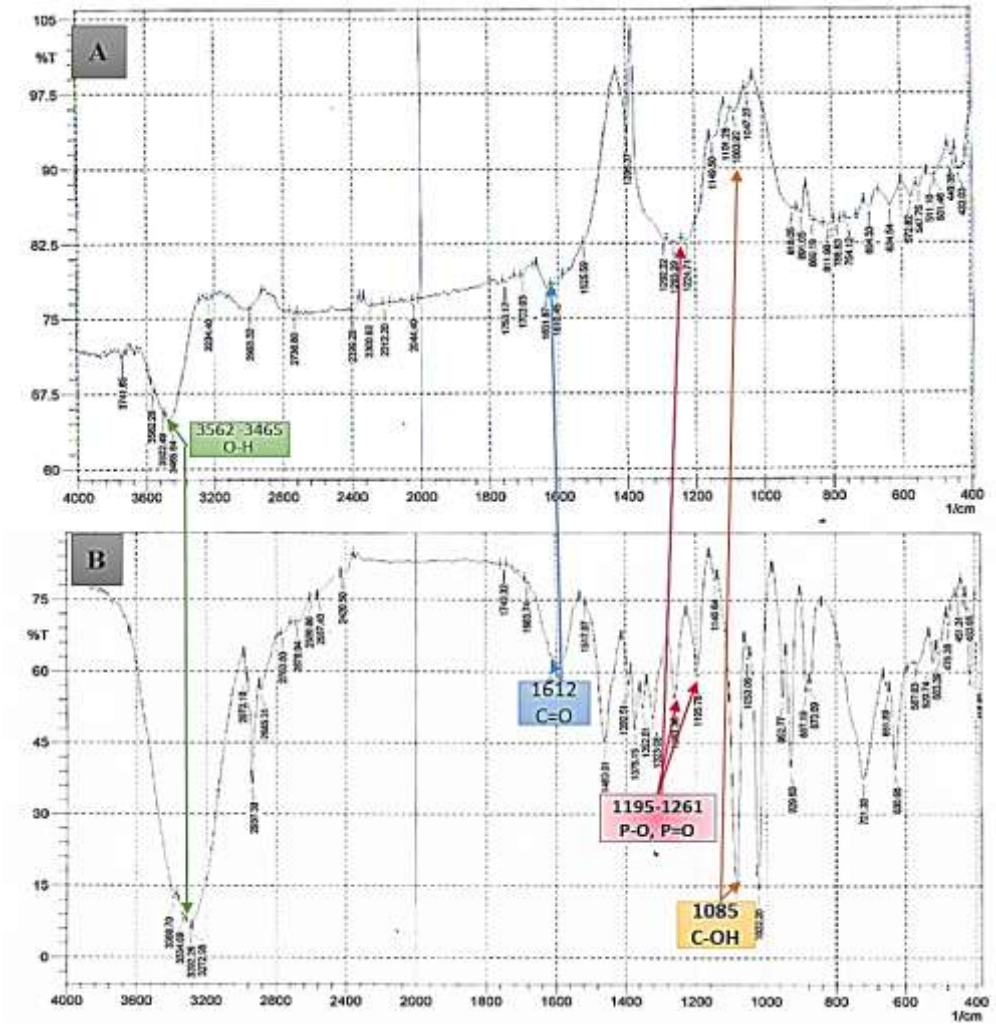

Figure 1: FTIR Scales for A: Graphene oxide, B: Zol-Go at the concentration ranging from (200 ng/ml to 11.7 ng/ml).

This was the same relationship that was found in the spectrum of GO. Additionally, Imidazole's CH=CH group vibrations are responsible for the bands at 1591 and 1612 cm-1, whereas the band at 962 cm-1 is attributable to the C-C bonds' stretching vibration. [47, 48]. The C-H bonds stretching vibrations in the ring of imidazole [21, 47-49] are responsible for the band that has a frequency of 1460 or 1392 cm1. The bands that were discovered at 1195 and 1261 cm-1 could have been caused by P-O bending vibrations and P=O bending vibrations, correspondingly [48]. In the spectra of ZOL-GO, besides ZOL band, there were two additional GO-related bands. These bands were found in the middle of the spectrum. There is a possibility that the C=O bending vibration from the GO carboxyl groups [43-46]was the cause of the 1612 cm-1 band. It is possible that the GO functional group (C-OH) is responsible for the appearance of the band at 1085 cm-1. The existence of these bands served as evidence that ZOL and GO had been conjugated. According to the results of the FTIR analysis, the drug complexes were successfully synthesized

Characterization of Zoledronic and Graphene oxide conjugation by UV-VIS spectroscopic analysis

The ZOL-GO conjugation was characterized via means of UV-vis spectrometry[1]. The UV-vis scales of zoledronic, graphene oxide, and zoledronic-graphene oxide are visualized in Figure 2. The peak of ZOL and GO are at a wavelength of 209 and 230 nm, correspondingly. The fact that ZOL was stacked on GO can be determined from the peaks that appeared in the UV-vis spectroscopy of coupled ZOL-GO. The peak of the UV-vis spectra of conjugated ZOL-GO that is connected to ZOL has shifted from 209 nm to 198 nm, indicating that it has been shifted. During this study, ZOL-GO complexes were created for the possible purpose of medication delivery.

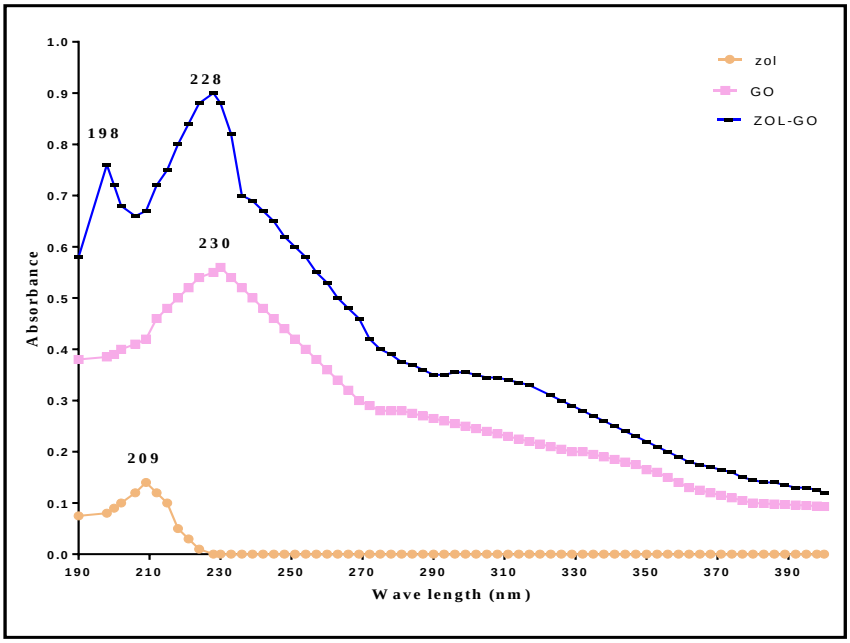

Figure 2: UV-Vis spectrophotometer, Absorbance for Zoledronic, Graphene oxide and Zol-Go recorded in aqueous solution.

According to the results of the FTIR analysis, the drug complexes were successfully synthesized. This observation provided confirmation for the findings of the study [1, 20] which demonstrated coupling of ZOL and GO through UV-vis spectroscopic analysis.

Atomic force microscope Analyses

AFM was applied to measure the superficial roughness, topography, as well as morphology (AFM). This approach gives atomic level 2D and 3D images of nanoparticles[50]. The 2D and 3D AFM pictures of ZOL-GO were presented in Figure 3, while Figure 4 revealed particle size distribution of ZOL-GO. AFM was used to measure the size of ZOL-GO nanoparticles as indicated in Table 2. According to the results, the average particle size of ZOL-GO was 73.23nm.

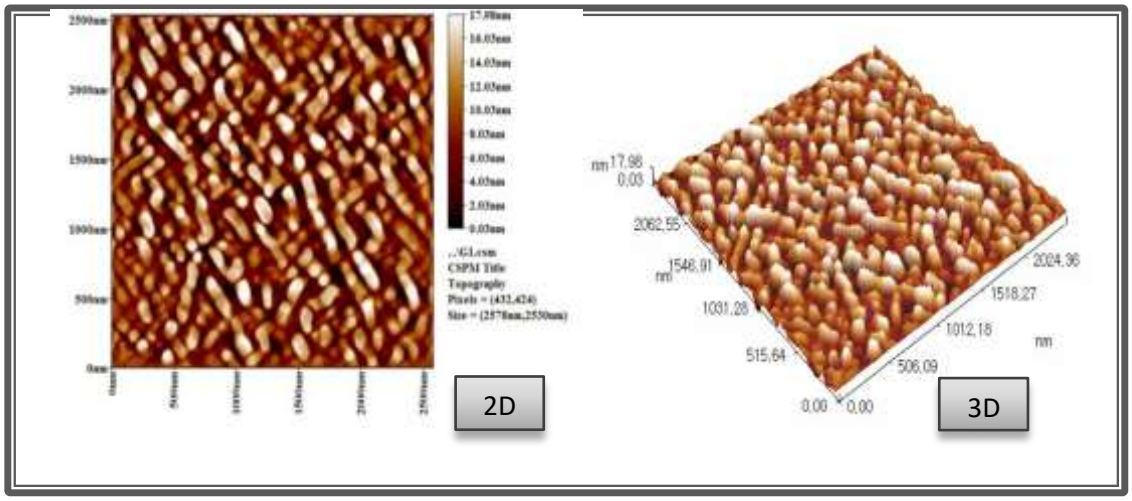

Figure 3: Nanoparticle ZOL-GO topologies shown in 2D and 3D using Atomic Force Microscopy.

Table 2: The findings of the AFM investigation of the ZOL-GO Average Size

Avg. Diameter:73.23 nm					**<=10% Diameter:45.00 nm**			
<=50% Diameter:65.00 nm					**<=90% Diameter:110.00 nm**			
Diameter(nm)<	Volume (%)	Cumulation (%)	Diameter(nm)<	Volume (%)	Cumulation (%)	Diameter(nm)<	Volume (%)	Cumulation (%)
45.00	9.98	9.98	90.00	3.27	75.86	135.00	0.54	96.73
50.00	12.34	22.32	95.00	4.17	80.04	140.00	0.54	97.28
55.00	7.44	29.76	100.00	3.63	83.67	145.00	0.73	98.00
60.00	8.35	38.11	105.00	2.54	86.21	150.00	0.54	98.55
65.00	9.80	47.91	110.00	2.36	88.57	160.00	1.09	99.64
70.00	7.80	55.72	115.00	2.90	91.47	165.00	0.18	99.82
75.00	6.90	62.61	120.00	2.36	93.83	175.00	0.18	100.00
80.00	5.81	68.42	125.00	1.45	95.28			
85.00	4.17	72.60	130.00	0.91	96.19			

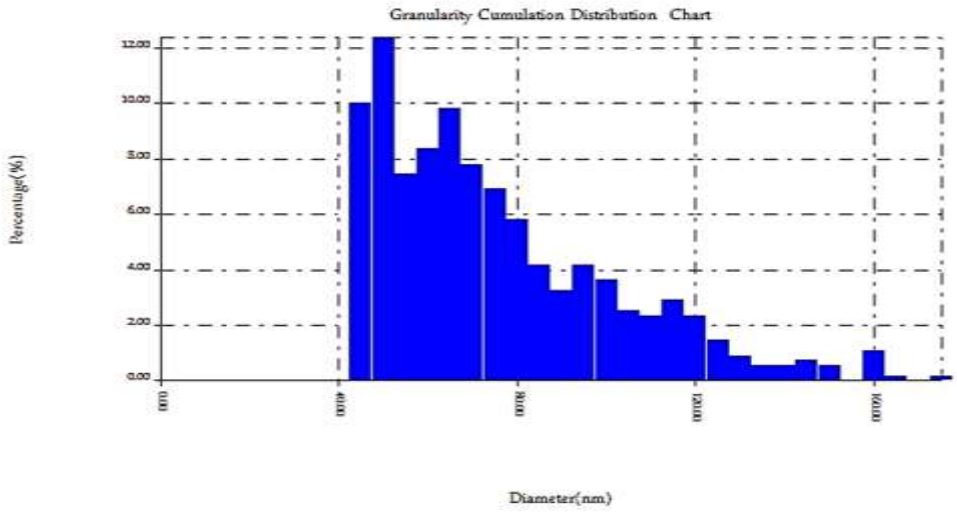

Figure 4: Distribution of ZOL-GO nanoparticles by particle size

The viability and morphology of PC3 prostate cancerous cells

MTT assay was used to test various concentrations of free GO, ZOL, and the conjugate ZOL-GO ranging from 10 to 1000 µg mL^{-1} for 24 hr. on prostate cancer cells (PC3) and normal cell lines (WRL 68). According to Figure 5, conjugated ZOL-GO is more cytotoxic than free GO and ZOL, both of which showed dose-dependent cytotoxicity. Free ZOL and GO have IC_{50} of 785.7 and 778.1 µg $mL^{-1,}$ respectively against PC3, while the IC_{50} of conjugated ZOL-GO was 787.9 against PC3.on the other hand the IC_{50} of GO, ZOL, and ZOL-GO conjugation against WRL68 were 841.8, 880.2 and 932.7, respectively. The cell viability of PC3 and WRL 68 at the IC_{50} concentration was 47.9% and 89% for PC3 cells and WRL68, respectively.

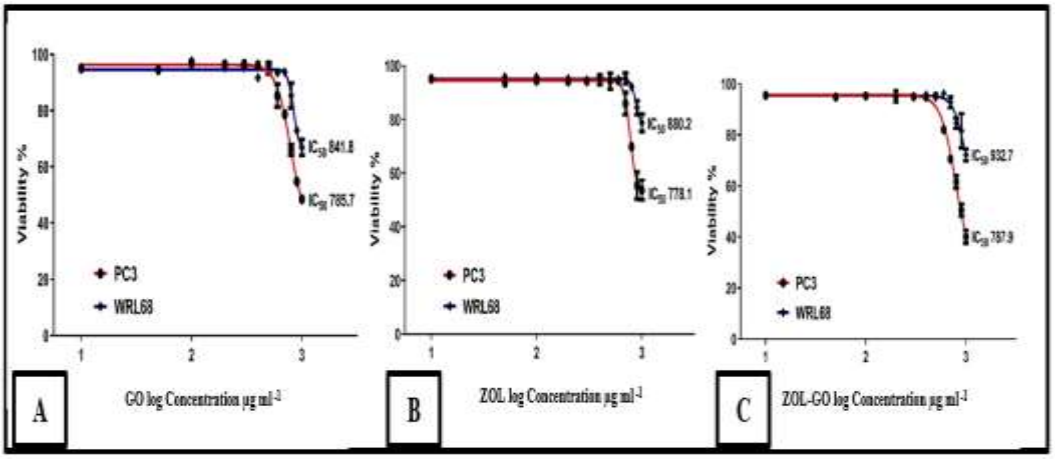

Figure 5: Cytotoxic effect of graphene-oxide loaded Zoledronic acid against human Prostate cancer (PC3) and human hepatic cells (WRL86) cell lines after 72 hr., incubation at 37ºC.using **A**: GO (graphene oxide), **B**: ZOL (Zoledronic acid), and **C**: conjugated ZOL-GO *: p-value ≤ 0.05- significant.

After treating WRL-68 with GO, ZOL, and conjugated ZOL-GO, all drugs showed moderate or low cytotoxic effects on normal cell lines. It is possible that ZOL-GO has a synergic effect, resulting in a lower PC3 cell survival percentage than would be achieved with the use of simply ZOL. Using an acridine orange analysis, Mohajeri et al.[51] found that conjugated ZOL-GO had this impact, as evidenced by the results; The presence of the GO

carrier most probably enhanced the drug's effectiveness. It was thought that absorption and cell permeation through the bilayer membrane were the two processes that were responsible for drug internalization in GO-affected cells. MCF-7 cells morphology changed when the ZOL-GO combination was utilized, which requires further investigation [51]. The ZOL-GO complexes tested on bone marrow-derived mesenchymal stem cells (BM-MSCs) with Alamar blue had no significant negative impact on those cells, according to the results of the study. Much other research [52-55] has also found that ZOL had no negative effects on BM-MSC viability; these results back up those other studies' conclusions. The ZOL and ZOL-GO combinations did not significantly diminish the survival of BM-MSCs; however, they drastically minimize the survival of MCF-7 cells, which is beneficial for such treatment of bone metastases[20].

Cell cycle analysis

A flow cytometer detected DNA following propidium iodide staining [56]. Cell cycle phase. An experiment was done to determine whether the decrease of PC3 cell viability by conjugated ZOL-GO was associated with cell cycle arrest.

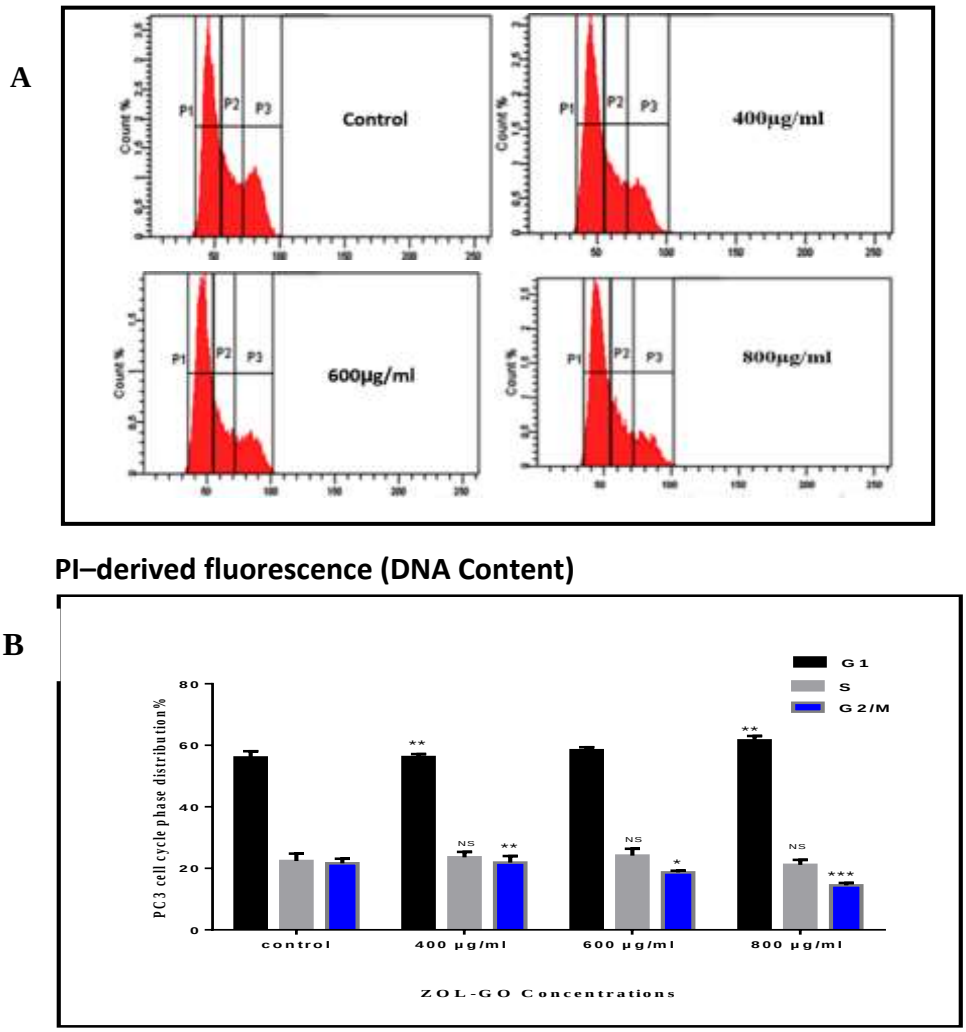

Figure 6: Influence of ZOL-GO on the distribution of prostate cancer cell line (PC3) cell cycle phase, **A:** Flow cytometry histogram has shown the distribution of PC3cell at different cell cycles (Gap 1, Synthesis, and Gap 2 / M) phases, used treatment control, 400, 600, and 800µg/mL for 24 hr., **B:** Mean cell counts differences at cell cycles (Gap 1, Synthesis, and Gap 2 / M) phases.

Using ZOL-GO at doses of 400, 600, and 800g/mL for 24 hours, the distribution of the cell cycle was determined. When ZOL-GO concentration was increased in a dose-dependent manner from 400 g/mL (56.2 percent) up to 800 g/mL (61.6 percent), the cell population increased significantly in the G1 phase, as shown in Figures (3-10) A and B, in comparison to the control with the p-value of around 0.002. ZOL-GO caused a high buildup of cells in the G1 phase, resulting in the expansion of cell percentage in the G1 phase, indicating G1 cell cycle arrest. We also saw a decrease in the number of cells within S+G2/M phase. However, at this stage, there were no notable changes in the S phase to go along with the rise of G1. At 800µg/mL, the G2/M population reduced by 14.5 percent in contrast to the control after 24 hours of treatment, with p-values as low as 0.0001 for both treatments. These data suggest that ZOL-GO may decrease the growth of PC3 cells by altering cell cycle regulators. Apoptosis and cell cycle arrest are regarded to be the most essential targets for creating anti-cancer medicines. It's possible that inhibiting the growth of tumor cells could lead to cell death through a process known as "programmed cell killing." According to the results of the flow cytometric study, ZOL-GO induced an accumulation of PC3 cells in the G1 phase in such a dose-dependent manner, suggesting that the movement from the G1 to S phase was prevented by ZOL-GO. This accumulation was mostly seen at 800µg/ml.

Conclusion

The influence of ZOL, GO, and conjugated ZOL-GO on WRL 68 and PC3 cell lines was examined. zoledronic and graphene oxide did not impact WRL 68 vitality. Based on the findings of our study, ZOL-GO that were evaluated shows a greater affinity for cancer cells than they do for normal cells. ZOL-GO exhibited cytotoxicity that varied with concentration. Additionally, the findings of this study demonstrated that ZOL-GO is a more cytotoxic substance than its base form ZOL demonstrated significantly increased cytotoxic effects against these cells by increasing apoptosis and interfering with cell cycle progression. Considering the rapidly developing field of graphene-based medicine, the findings that we have provided in this study have the potential to perform a vital part in the growth of future applications of ZOL-GO in the treatment of prostate cancer and metastasis treatments.

ETHICAL CLEARANCE

The Research Ethical Committee at scientific research by ethical approval of both environmental and health and higher education and scientific research ministries in Iraq.

CONFLICT OF INTEREST

The authors declare that they have no conflict of interest.

References

[1] S. Tavakoli and D. Ege, "Graphene Oxide as a drug carrier for delivery of zoledronic acid in secondary bone cancer treatment," *MRS Advances*, vol. 4, no. 21, pp. 1231-1236, 2019.

[2] P. Clézardin *et al.*, "Bone metastasis: Mechanisms, therapies, and biomarkers," *Physiological reviews*, vol. 101, no. 3, pp. 797-855, 2021.

[3] L. Ambrosio, M. G. Raucci, G. Vadalà, L. Ambrosio, R. Papalia, and V. Denaro, "Innovative biomaterials for the treatment of bone cancer," *International Journal of Molecular Sciences*, vol. 22, no. 15, p. 8214, 2021.

[4] A. Ali *et al.*, "Association of bone metastatic burden with survival benefit from prostate radiotherapy in patients with newly diagnosed metastatic prostate cancer: a secondary analysis of a randomized clinical trial," *JAMA oncology*, vol. 7, no. 4, pp. 555-563, 2021.

[5] Z. Mbese and B. A. Aderibigbe, "Bisphosphonate-Based Conjugates and Derivatives as Potential Therapeutic Agents in Osteoporosis, Bone Cancer and Metastatic Bone Cancer," *International Journal of Molecular Sciences*, vol. 22, no. 13, p. 6869, 2021.

[6] A. Schmid-Alliana, H. Schmid-Antomarchi, R. Al-Sahlanee, P. Lagadec, J.-C. Scimeca, and E. Verron, "Understanding the progression of bone metastases to identify novel therapeutic targets," *International journal of molecular sciences*, vol. 19, no. 1, p. 148, 2018.

[7] Y. Xu *et al.*, "Zoledronic Acid-loaded hybrid hyaluronic acid/polyethylene glycol/nano-hydroxyapatite nanoparticle: novel fabrication and safety verification," *Frontiers in bioengineering and biotechnology*, vol. 9, p. 629928, 2021.

[8] M.-X. Ren *et al.*, "Magnetite nanoparticles anchored on graphene oxide loaded with doxorubicin hydrochloride for magnetic hyperthermia therapy," *Ceramics International*, vol. 47, no. 14, pp. 20686-20692, 2021.

[9] F. Macedo *et al.*, "Bone metastases: an overview," *Oncology reviews*, vol. 11, no. 1, 2017.

[10] E. Svensson, C. F. Christiansen, S. P. Ulrichsen, M. R. Rørth, and H. T. Sørensen, "Survival after bone metastasis by primary cancer type: a Danish population-based cohort study," *BMJ open*, vol. 7, no. 9, p. e016022, 2017.

[11] Y. Zhong and S. Li, "New Progress in Improving the Delivery Methods of Bisphosphonates in the Treatment of Bone Tumors," *Drug Design, Development and Therapy*, vol. 15, p. 4939, 2021.

[12] S. Junankar and M. J. Rogers, "Cellular and molecular actions of bisphosphonates," in *Bone Cancer*: Elsevier, 2015, pp. 615-627.

[13] R. A. Nadar, N. Margiotta, M. Iafisco, J. J. van den Beucken, O. C. Boerman, and S. C. Leeuwenburgh, "Bisphosphonate-functionalized imaging agents, anti-tumor agents and nanocarriers for treatment of bone cancer," *Advanced healthcare materials*, vol. 6, no. 8, p. 1601119, 2017.

[14] B. Torger, D. Vehlow, B. Urban, S. Salem, D. Appelhans, and M. Müller, "Cast adhesive polyelectrolyte complex particle films of unmodified or maltose-modified poly (ethyleneimine) and cellulose sulphate: fabrication, film stability and retarded release of zoledronate," *Biointerphases*, vol. 8, no. 1, p. 25, 2013.

[15] S. Patntirapong, W. Singhatanadgit, C. Chanruangvanit, K. Lavanrattanakul, and Y. Satravaha, "Zoledronic acid suppresses mineralization through direct cytotoxicity and osteoblast differentiation inhibition," *Journal of oral pathology & medicine*, vol. 41, no. 9, pp. 713-720, 2012.

[16] [16] J. Seo, S. Jeong, M. Lee, and T.-i. Kim, "Zoledronic acid-loaded cationic methylcellulose polyplex nanoparticles for enhanced gene delivery efficiency and breast cancer cell killing effect," *Applied Nanoscience*, pp. 1-12, 2022.

[17] S. A. Holstein, "A patent review of bisphosphonates in treating bone disease," *Expert opinion on therapeutic patents*, vol. 29, no. 5, pp. 315-325, 2019.

[18] A. Göbel *et al.*, "Combined inhibition of the mevalonate pathway with statins and zoledronic acid potentiates their anti-tumor effects in human breast cancer cells," *Cancer Letters*, vol. 375, no. 1,

[19] M. A. Jara, J. Varghese, and M. I. Hu, "Adverse events associated with bone-directed therapies in patients with cancer," *Bone*, p. 115901, 2021.

[20] G. Boran, S. Tavakoli, I. Dierking, A. R. Kamali, and D. Ege, "Synergistic effect of graphene oxide and zoledronic acid for osteoporosis and cancer treatment," *Scientific reports*, vol. 10, no. 1, pp. 1-12, 2020.

[21] D. K. Khajuria, R. Vasireddi, M. Trebbin, D. Karasik, and R. Razdan, "Novel therapeutic intervention for osteoporosis prepared with strontium hydroxyapatite and zoledronic acid: In vitro and pharmacodynamic evaluation," *Materials Science and Engineering: C*, vol. 71, pp. 698-708, 2017.

[22] W. Gou *et al.*, "Controlled delivery of zoledronate improved bone formation locally in vivo," *PLoS One*, vol. 9, no. 3, p. e91317, 2014.

[23] A. A. Khan, M. Jabeen, I. Hassan, M. Furqan, and A. M. Alanazi, "Lipid Nanosystems: Targeted Nano-delivery of Therapeutic Agents in Treatment of Cancer," in *Functional Lipid Nanosystems in Cancer*: Jenny Stanford Publishing, 2021, pp. 351-377.

[24] A. Kadow-Romacker, S. Greiner, G. Schmidmaier, and B. Wildemann, "Effect of β-tricalcium phosphate coated with zoledronic acid on human osteoblasts and human osteoclasts in vitro," *Journal of biomaterials applications*, vol. 27, no. 5, pp. 577-585, 2013.

[25] D. B. Raina, H. Isaksson, W. Hettwer, A. Kumar, L. Lidgren, and M. Tägil, "A biphasic calcium sulphate/hydroxyapatite carrier containing bone morphogenic protein-2 and zoledronic acid generates bone," *Scientific reports*, vol. 6, no. 1, pp. 1-13, 2016.

[26] D. B. Raina *et al.*, "Gelatin-hydroxyapatite-calcium sulphate based biomaterial for long term sustained delivery of bone morphogenic protein-2 and zoledronic acid for increased bone formation: In-vitro and in-vivo carrier properties," *Journal of controlled release*, vol. 272, pp. 83-96, 2018.

[27] Z. Liu, J. T. Robinson, S. M. Tabakman, K. Yang, and H. Dai, "Carbon materials for drug delivery & cancer therapy," *Materials today*, vol. 14, no. 7-8, pp. 316-323, 2011.

[28] D.-J. Lim, M. Sim, L. Oh, K. Lim, and H. Park, "Carbon-based drug delivery carriers for cancer therapy," *Archives of pharmacal research*, vol. 37, no. 1, pp. 43-52, 2014.

[29] J. S. Stefano *et al.*, "Electrochemical detection of 2, 4, 6-trinitrotoluene on carbon nanotube modified electrode: Effect of acid functionalization," *Journal of Solid State Electrochemistry*, vol. 24, no. 1, pp. 121-129, 2020.

[30] R. Zhang and H. Olin, "Carbon nanomaterials as drug carriers: Real time drug release investigation," *Materials Science and Engineering: C*, vol. 32, no. 5, pp. 1247-1252, 2012.

[31] N. G. Sahoo *et al.*, "Functionalized carbon nanomaterials as nanocarriers for loading and delivery of a poorly water-soluble anticancer drug: a comparative study," *Chemical communications*, vol. 47, no. 18, pp. 5235-5237, 2011.

[32] D. Ege, A. R. Kamali, and A. R. Boccaccini, "Graphene oxide/polymer-based biomaterials," *Advanced Engineering Materials*, vol. 19, no. 12, p. 1700627, 2017.

[33] E. Quagliarini, R. Di Santo, D. Pozzi, P. Tentori, F. Cardarelli, and G. Caracciolo, "Mechanistic insights into the release of doxorubicin from graphene oxide in cancer cells," *Nanomaterials*, vol. 10, no. 8, p. 1482, 2020.

[34] J. Wu *et al.*, "Graphene oxide used as a carrier for adriamycin can reverse drug resistance in breast cancer cells," *Nanotechnology*, vol. 23, no. 35, p. 355101, 2012.

[35] N. A. Hussien, N. Işıklan, and M. Türk, "Pectin-conjugated magnetic graphene oxide nanohybrid as a novel drug carrier for paclitaxel delivery," *Artificial cells, nanomedicine, and biotechnology*, vol. 46, no. sup1, pp. 264-273, 2018.

[36] L. Yang, F. Wang, H. Han, L. Yang, G. Zhang, and Z. Fan, "Functionalized graphene oxide as a drug carrier for loading pirfenidone in treatment of subarachnoid hemorrhage," *Colloids and Surfaces B: Biointerfaces*, vol. 129, pp. 21-29, 2015.

[37] S. Gautam, "Graphene oxide: a potential drug carrier for cancer therapy," *Research and Reviews: A Journal of Pharmaceutical Science*, vol. 8, pp. 21-31, 2017.

[38] A. Najmafshar, M. Rostami, J. Varshosaz, D. Norouzian, and S. Z. A. Samsam Shariat, "Enhanced antitumor activity of bovine lactoferrin through immobilization onto functionalized nano graphene oxide: an in vitro/in vivo study," *Drug delivery*, vol. 27, no. 1, pp. 1236-1247, 2020.

[39] R. I. Freshney, *Culture of animal cells : a manual of basic technique and specialized applications*. Hoboken, N.J.: Wiley-Blackwell, 2010.

[40] A. A. A. Al-Ali, K. A. S. Alsalami, and A. M. Athbi, "Cytotoxic effects of CeO2 NPs and β-Carotene and their ability to induce apoptosis in human breast normal and cancer cell lines," *Iraqi Journal of Science*, vol. 63, no. 3, pp. 923-937, 03/30 2022.

[41] E. Ulukaya, D. Karakas, and K. Dimas, "Tumor chemosensitivity assays are helpful for personalized Cytotoxic treatments in cancer patients," *Medicina*, vol. 57, no. 6, p. 636, 2021.

[42] X.-Y. Ge, L.-Q. Yang, Y. Jiang, W.-W. Yang, J. Fu, and S.-L. Li, "Reactive oxygen species and autophagy associated apoptosis and limitation of clonogenic survival induced by zoledronic acid in salivary adenoid cystic carcinoma cell line SACC-83," *PLoS One*, vol. 9, no. 6, p. e101207, 2014.

[43] X. Zhang, W. Hu, J. Li, L. Tao, and Y. Wei, "A comparative study of cellular uptake and cytotoxicity of multi-walled carbon nanotubes, graphene oxide, and nanodiamond," *Toxicology Research*, vol. 1, no. 1, pp. 62-68, 2012.

[44] C. Manoratne, S. Rosa, and I. Kottegoda, "XRD-HTA, UV visible, FTIR and SEM interpretation of reduced graphene oxide synthesized from high purity vein graphite," *Mater. Sci. Res. India*, vol. 14, no. 1, pp. 19-30, 2017.

[45] J. Paredes, S. Villar-Rodil, A. Martínez-Alonso, and J. M. Tascon, "Graphene oxide dispersions in organic solvents," *Langmuir*, vol. 24, no. 19, pp. 10560-10564, 2008.

[46] J. Q. Jiang, S. Ashekuzzaman, J. S. Hargreaves, A. R. McFarlane, A. B. M. Badruzzaman, and M. H. Tarek, "Removal of Arsenic (III) from groundwater applying a reusable Mg-Fe-Cl layered double hydroxide," *Journal of Chemical Technology & Biotechnology*, vol. 90, no. 6, pp. 1160-1166, 2015.

[47] D. K. Khajuria, R. Razdan, and D. R. Mahapatra, "Development, in vitro and in vivo characterization of zoledronic acid functionalized hydroxyapatite nanoparticle based formulation for treatment of osteoporosis in animal model," *European Journal of Pharmaceutical Sciences*, vol. 66, pp. 173-183, 2015.

[48] M. Prasanthi, B. Rao, B. Rao, Y. Krishna, and D. Ramana, "Formulation and evaluation of zoledronic acid for injection by lyophilization technique," *Int. Res. J. Pharm*, vol. 8, pp. 50-56, 2017.

[49] S. Chen, P. Wan, B. Zhang, K. Yang, and Y. Li, "Facile fabrication of the zoledronate-incorporated coating on magnesium alloy for orthopaedic implants," *Journal of Orthopaedic Translation*, vol. 22, pp. 2-6, 2020.

[50] W. N. Alsaady and I. A. Zaidan, "The synergistic effects of chitosan-alginate nanoparticles loaded with doxycycline antibiotic against multidrug resistant proteus mirabilis, Escherichia coli and enterococcus faecalis," *Iraqi Journal of Science*, pp. 3187-3199, 2020.

[51] M. Mohajeri, B. Behnam, and A. Sahebkar, "Biomedical applications of carbon nanomaterials: Drug and gene delivery potentials," *Journal of cellular physiology*, vol. 234, no. 1, pp. 298-319, 2019.

[52] A. Schindeler and D. G. Little, "Osteoclasts but not osteoblasts are affected by a calcified surface treated with zoledronic acid in vitro," *Biochemical and biophysical research communications*, vol. 338, no. 2, pp. 710-716, 2005.

[53] R. R. Recker *et al.*, "Effects of intravenous zoledronic acid once yearly on bone remodeling and bone structure," *Journal of Bone and Mineral Research*, vol. 23, no. 1, pp. 6-16, 2008.

[54] R. Ebert *et al.*, "Pulse treatment with zoledronic acid causes sustained commitment of bone marrow derived mesenchymal stem cells for osteogenic differentiation," *Bone*, vol. 44, no. 5, pp. 858-864, 2009.

[55] B. Peter *et al.*, "Calcium phosphate drug delivery system: influence of local zoledronate release on bone implant osteointegration," *Bone*, vol. 36, no. 1, pp. 52-60, 2005.

[56] Y. Shen, P. Vignali, and R. Wang, "Rapid Profiling Cell Cycle by Flow Cytometry Using Concurrent Staining of DNA and Mitotic Markers," (in eng), *Bio Protoc*, vol. 7, no. 16, Aug 20 2017.